PAPER

Check for updates

Magnetic Fe₃O₄@silica sulfuric acid nanoparticles promoted regioselective protection/deprotection of alcohols with dihydropyran under solvent-free conditions†

Kalyani Rajkumari, Juri Kalita, Diparjun Das and Samuel Lalthazuala Rokhum [iD] *

Protection (and deprotection) of hydroxyl groups *via* tetrahydropyranylation was carried out effectively using a catalytic amount of Fe_3O_4 supported silica sulphuric acid nanoparticles ($Fe_3O_4@SiO_2@SO_3H$) under solvent-free conditions. The synthesized nanocatalyst was characterized by XRD, TEM, FT-IR *etc.* A wide range of tetrahydropyranylated alcohol derivatives were synthesized using this heterogeneous magnetic nanocatalyst within 10–20 min with high yields. In addition, tetrahydropyranyl ethers could also be deprotected to the parent alcoholic compounds in the presence of MeOH using the same catalyst. After completion of the reactions, the catalyst was easily separated from the reaction medium using an external magnet, which ameliorated the overall synthetic process. The catalyst was recovered and reused for five successive reactions without any appreciable loss in its activity. Mild reactions conditions, operational simplicity, solvent free conditions, high selectivity, easy recyclability of the magnetic nanocatalyst, and high yields can be considered as the advantageous features of our procedure.

1. Introduction

During the synthesis of an organic compound, the protection (and deprotection) of the free hydroxyl group in a multifunctional alcohol substrate or intermediate is one of the most frequently used strategies.[1,2] For this type of functional manipulation, etherification of the hydroxyl group using 3,4-dihydro-2H-pyran (DHP) is recognized as the most popular and easy protocol. This is because of its several attractive advantages over other protecting reagents, which include ease of its preparation, stability of the corresponding tetrahydropyranyl ethers towards various reaction conditions and use of reagents such as strong bases, hydrides, Grignard reagents and other organometallic reagents.[3–5] Moreover, THP ethers can easily be converted to various derivatives, such as sulfides, halides,[6] esters,[7] cyanides and carbonyl compounds[8] employing specific methods, which makes them ideal protecting reagents for tetrahydropyranylation.

Enumerable catalysts including both homogeneous and heterogeneous catalysts have been reported to date, which have been proposed to catalyze tetrahydropyranylation of free hydroxyl groups. Taking into account the advantages of heterogeneous catalysts over homogeneous catalysts in terms of

separation and recoverability, several effective heterogeneous catalysts have been reported in recent years.[9,10] However a serious disadvantage of heterogeneous catalysts is that their efficiency gets restricted due to the limited surface area.[11] This drawback can be overcome by a nanoporous catalyst support due to its "plenty of room at the bottom" nature, which can also be considered as a bridge between heterogeneous and homogenous catalysts.[12]

In recent decades, magnetic nanoparticles (MNPs) have gained enormous attention since they can be easily separated from the reaction medium by an external magnet, preventing the use of column chromatography, avoiding loss of product, enhancing recyclability and thus ameliorating the overall synthesis process.[13] Magnetic Fe_3O_4 has been investigated the most due to its potential magnetic nature although bare iron oxide nanoparticles have several limitations, which include immediate aggregation into large clusters and rapid exothermic reactions with oxygen.[14,15] However surface modification by forming a silica coating over the MNP surface can make it stable, inert, non-toxic, resistant under catalytic conditions as well as improve the surface functionality due to the availability of abundant silanol groups (–SiOH), which act as a support for immobilization of the SO_3H function. Owing to the unique properties of magnetic nanoparticles, sulphuric acid adsorbed on silica coating MNPs core–shell structures ($Fe_3O_4@SiO_2@$-SO_3H) have been utilized as a catalyst in various organic transformations, such as Biginelli reaction,[16] synthesis of amidoalkyl naphthols[17] and protection–deprotection of hydroxyl

Department of Chemistry, National Institute of Technology, Silchar-788010, Assam, India. E-mail: rokhum@che.nits.ac.in; Fax: +91 3842 224797; Tel: +91 3842 242915

† Electronic supplementary information (ESI) available: ¹H and ¹³C NMR spectra of synthesized compounds. See DOI: 10.1039/c7ra12458a

groups using hexamethyldisilazane (HMDS).[18] In this communication, we report tetrahydropyranylation/depyranylation of alcohols with sulphuric acid adsorbed on a silica coating MNPs core–shell structure under solvent-free conditions, which makes it free from the hazardous effects of organic toxic solvents, offering a green and eco-friendly approach.

2. Experimental methodology

2.1 Materials and methods

All alcohols, DHP (3,4-dihydro-2H-pyran), silica gel for TLC (Thin Layer Chromatography) and column chromatography were of analytical grade and purchased from SpectroChem. TEOS (tetraethyl orthosilicate) was purchased from Sigma Aldrich, India. The chemicals were used without further purification. The solvent used were of extra pure grade, purchased from Merck India. Double distilled deionized water was used for the synthesis of magnetic nanoparticles.

For characterization of the catalyst, high resolution transmission electron microscopy (HRTEM) was conducted using an electron microscope JEM-2100, 200 kV, JEOL (SAIF-NEHU, Shillong). The samples were dispersed in ethanol, DCM (dichloromethane) and then treated ultrasonically in order to disperse individual particles over a copper grid. Powder X-Ray Diffraction (XRD) patterns were obtained on an X'Pert Pro PANalytical diffractometer (SAIF-GU, Guwahati) under the following conditions: K-Alpha 1 wavelength ($\lambda = 1.54056$ Å), K-Alpha 2 wavelength ($\lambda = 1.54439$ Å), generator voltage of 40 kV, a tube current of 35 mA and the count time of 0.5 s per 0.02° in the range of 5°–90° with a copper anode. FTIR spectra were recorded on a Nicolet 6700, Nicolet Continuum FTIR Microscope (IASST, Guwahati). NMR spectra were recorded on Bruker Avance II, 400 MHz (SAIF NEHU, Shillong).

2.2 Preparation of catalysts

2.2.1 Preparation of iron oxide magnetic nanoparticles, Fe$_3$O$_4$ MNPs. Magnetic nanoparticles were synthesized according to a reported procedure.[19–21] Co-precipitation of Fe(II) and Fe(III) was carried out by first dissolving FeCl$_2\cdot$4H$_2$O (1 mmol) and FeCl$_3\cdot$6H$_2$O (2 mmol) in deionized water under a nitrogen atmosphere at 90 °C. Ammonium hydroxide solution was added to the above solution with vigorous mechanical stirring. The reaction was carried out for 60 min in under N$_2$ atmosphere until the color of the bulk solution turned black. An external magnet was used to separate out the resulting black MNPs, washed 3 times with deionized water and then dried under vacuum at 60 °C for 12 h.

2.2.2 Preparation of the silica coating of iron oxide magnetic nanoparticles, Fe$_3$O$_4$@SiO$_2$. Silica coating of Fe$_3$O$_4$ MNPs was carried out using a sol–gel method (Stober method) that involves hydrolysis of TEOS on the surface of iron oxide nanospheres. For this, Fe$_3$O$_4$ particles were dispersed in a mixture of ethanol, deionized water and TEOS, followed by the addition of 10% NaOH solution. The solution was stirred using a magnetic stirrer for about 1 h at room temperature. Then, the product was isolated by an external magnet and was washed

several times with deionized water and ethanol and dried at 80 °C for 10 h under vacuum (24 mmHg). The thickness of the coated silica can be controlled by tuning the experimental parameters.

2.2.3 Preparation of SO$_3$H functionalized silica-coated iron oxide magnetic nanoparticles; Fe$_3$O$_4$ supported silica sulfonic acid (Fe$_3$O$_4$@SiO$_2$@SO$_3$H). To immobilize the SO$_3$H functional group onto the surface of Fe$_3$O$_4$@SiO$_2$ nanoparticles, a suction flask equipped with a constant pressure dropping funnel was used. The gas outlet was connected to a vacuum system through an absorbing solution of alkali trap for conducting HCl gas. Fe$_3$O$_4$@SiO$_2$ was dispersed into the flask containing dry DCM. Chlorosulfonic acid (ClSO$_3$H) was then added dropwise to the mixture of Fe$_3$O$_4$@SiO$_2$ and DCM in a cooled ice-bath over a period of 30 min at room temperature. HCl gas evolved from the reaction vessel immediately. After completion of the addition, the mixture was stirred and occasionally shaken for 3 h, while the residual HCl was eliminated by suction. Then, Fe$_3$O$_4$@silica sulfonic acid was separated from the reaction mixture by an external magnet and washed several times with DCM. Finally, Fe$_3$O$_4$@silica sulfonic acid was dried under vacuum at 60 °C for 24 h (Scheme 1).

2.3 General procedure for the tetrahydropyranylation of alcohols using Fe$_3$O$_4$@silica sulfonic acid (Fe$_3$O$_4$@SiO$_2$@SO$_3$H)

A mixture of alcohol (1 mmol), DHP (1.2 mmol) and Fe$_3$O$_4$@silica sulfonic acid catalyst (0.15 g, 20 mol% of substrate) was stirred in a small reaction vessel at room temperature. The reaction progress was monitored by thin layer chromatography. After completion of the reaction, ethyl acetate (10 mL) was added to the solution and the catalyst was separated by an external magnet. The solution was concentrated under reduced pressure and the product was passed through a column of silica gel eluting with hexane/ethyl acetate (9 : 1) to obtain pure THP ether with high purity. The catalyst was washed several times with ethyl acetate and dried under vacuum (24 mmHg) at 60 °C for 24 h.

2.4 General procedure for the deprotection of alcohols

THP ether (1 mmol) and Fe$_3$O$_4$@silica sulfonic acid catalyst (20 mol% of substrate) were stirred in methanol (0.5 mL) at
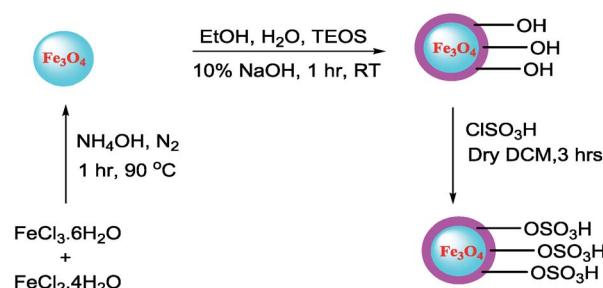
Scheme 1 Schematic diagram for synthesis of Fe$_3$O$_4$@silica sulfonic acid nanocatalyst.

room temperature for 30 min. The cleavage of THP ethers was monitored by TLC. After completion of the reaction, the catalyst was separated with the help of an external magnet and washed with ethyl acetate. The solution was concentrated under reduced pressure to obtain the corresponding pure hydroxyl compound in a quantitative yield.

3. Result and discussion

3.1 Catalyst characterization

The synthesized Fe_3O_4@silica sulfonic acid nanoparticles were characterized by Fourier Transform Infrared (FT-IR) spectroscopy, X-Ray Diffraction and Transmission Electron Microscopy (TEM).

3.1.1 Fourier transform infrared (FT-IR) spectroscopy. The FT-IR spectra of pure Fe_3O_4, Fe_3O_4@SiO_2 core–shell, and Fe_3O_4@silica sulfonic acid nanoparticles are shown in Fig. 1(a)–(c), respectively.

The absorption peak at approximately 579 cm^{-1} (Fig. 1(a)) corresponds to the stretching vibration of the Fe–O bond[17] and the adsorption of the silica coating on the magnetite surface was indicated by the band near 1031 and 893 cm^{-1}, which are assigned to the Si–O stretching vibration (Fig. 1(b)). In addition, successful sulfonic acid functionalization of the silica layer on Fe_3O_4 surface was evidenced by the absorption bands at 1076 cm^{-1} and 1136 cm^{-1} related to the stretching of the S–O bonds. A peak appeared at about 3402 cm^{-1} due to the stretching of the OH groups in the SO_3H moiety (Fig. 1(c)). These FT-IR spectra provided evidence of the formation of a silica shell onto the surface of Fe_3O_4 and the acid functionalization of the silica shell.[17,18]

3.1.2 X-ray diffraction (XRD). The structure of (a) Fe_3O_4 and (b) Fe_3O_4@SiO_2 was analyzed by XRD spectroscopy (Fig. 2). The XRD pattern of the bare Fe_3O_4 NPs shows diffraction peaks at 2θ values 30.2°, 35.6°, 43.4°, 54°, 57.3° and 63.1° corresponding to the (2 2 0), (3 1 1), (4 0 0), (4 2 2), (5 1 1) and (4 4 0) planes. This suggests an inverse spinal structure for the magnetic crystal and matched well with the library patterns (JCPDS no. 19-0629). The
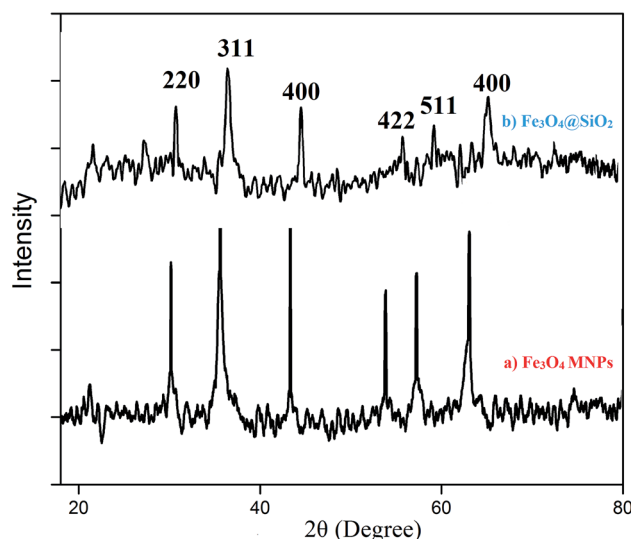

Fig. 2 XRD spectra of (a) Fe_3O_4, (b) Fe_3O_4@silica sulfonic acid.

peaks for Fe_3O_4@silica were same as that of Fe_3O_4 MNPs, which firmly indicates retention of the crystalline inverse cubic spinel structure during the silica-coating process. The broad peak appearing in the range of $2\theta = 15$–30 (Fig. 2) is the characteristic peak of amorphous silica.

3.1.3 Transmission electron microscopy. The size and shape of Fe_3O_4 nanoparticles and the prepared catalyst were examined by TEM. Fig. 3(a) and (b) show the TEM images of the Fe_3O_4 nanoparticles at different magnifications. It can be observed that formation of 'quasi-spherical' shaped nanoparticles have taken place (Fig. 3(a)). Magnetite particles of diameter 17.68 nm can be observed.
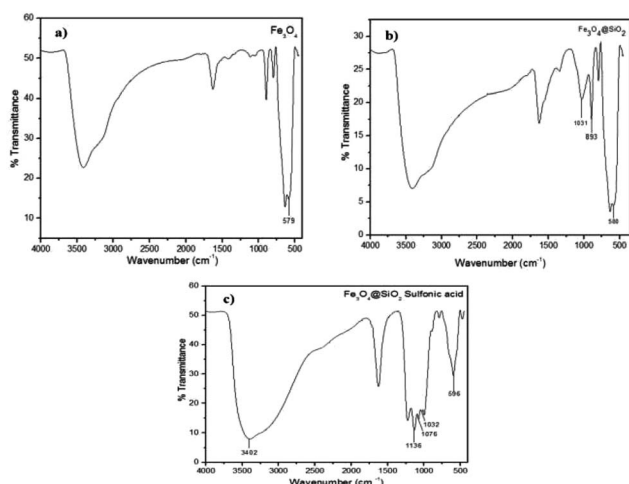

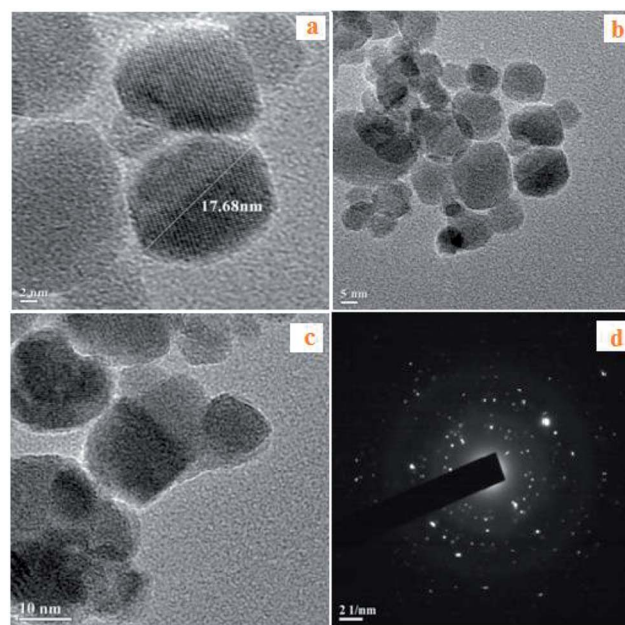Fig. 1 FT IR spectra of (a) Fe_3O_4, (b) Fe_3O_4@SiO_2 and (c) Fe_3O_4@silica sulfonic acid.

Fig. 3 (a) HRTEM images of Fe_3O_4 nanoparticles, (b) HRTEM images of Fe_3O_4@SiO_2, (c) HRTEM images of Fe_3O_4@SiO_2@SO_3H, (d) ED pattern of Fe_3O_4@SiO_2@SO_3H.

The fine coating of silica over the Fe_3O_4 nanoparticles can be observed from the TEM images shown in Fig. 3(b) and (c), which indicates the retention of the silica coating even after the sulfonic acid functionalization on the silica surface.[17,19]

Further, the SAED (Selected Area Electron Diffraction) pattern (Fig. 3(d)) of the Fe_3O_4 nanoparticles confirms that the sample is crystalline and also confirms our conclusions from the X-ray diffraction pattern.

3.2   Protection and deprotection of alcohols

In continuation of our ongoing research interest, we applied the synthesized catalyst in tetrahydropyranylation of various alcohol substituents. Initially, we tried it with benzyl alcohol and, to our delight; protection of alcohol was successful under solvent-free conditions within a very short time of 1 h only. First, we took an equimolar mixture of benzyl alcohol (1 mmol) and DHP (1 mmol) and 10 mol% of the nanocatalyst and stirred the mixture for 1 h. After stirring for 1 h, we observed only slight formation of the product as indicated by TLC. Surprisingly, this did not increase even after stirring for another 1 h. Then, we added additional DHP (0.2 mmol) and found that the reaction was completed within the next 1 h. Inspired by these findings, our next evident target was to optimize the amount of catalyst. To our satisfaction, we found that 20 mol% of the nanocatalyst was optimum for the protection of alcohols (Table 1, entry 4).

Encouraged by the result and the advantage of using magnetic nanocatalysts over soluble homogeneous catalysts, we carried out the conversion of various alcohols into their protected products as described in Scheme 2.

With the optimum reaction condition in hand, we carried out the tetrahydropyranylation of a variety of primary, secondary, tertiary, benzylic and allylic alcohols which were smoothly converted to the corresponding desired products in good to excellent yields at room temperature. It was observed that benzylic alcohols substituted with electron-donating groups are highly reactive under our reaction condition,

giving the corresponding protected alcohols in excellent yields (Table 2, entries 2 and 3). However, reactions of benzyl alcohols substituted with electron-withdrawing groups were, to some extent, slower as compared to their electron-donating counterparts (Table 2, entry 5). Although the reaction rates of aliphatic alcohols were lower as compared to the benzylic ones, they were easily converted into their corresponding products in high yields. It was observed that aliphatic alcohols with larger chain lengths take more time for completion than those with smaller chain lengths (Table 2, entries 7, 8, and 9). However, secondary and tertiary alcohols took longer time for complete conversion (Table 2, entries 11 and 12). Allyl alcohols (Table 2, entries 13 and 14) were converted into the corresponding protected alcohols leaving the olefinic bonds intact.

Table 1   Optimization of the catalyst[a]

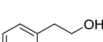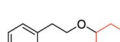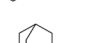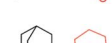| Entry	Catalyst amount (mol%)	Time (min)	Yield (%)
1	5	150	65
2	10	120	85
3	15	55	90
4	20	45	95
5	25	45	95
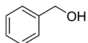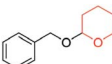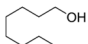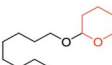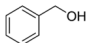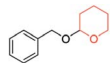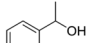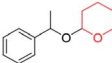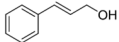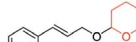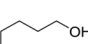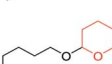
[a] Reaction conditions: benzyl alcohol (1 mmol), DHP (1.2 mmol), room temperature, solvent-free condition.

Scheme 2 Tetrahydropyranylation of alcohols using 20 mol% of nanocatalyst.
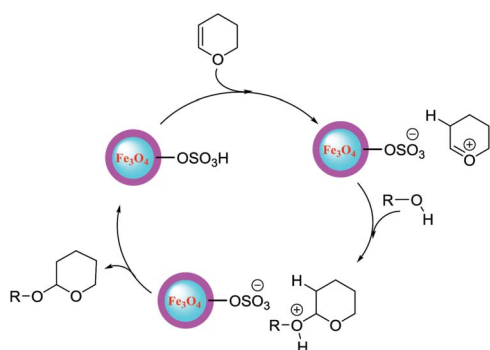
Table 2   Tetrahydropyranylation of alcohols[a]

Entry	Alcohols	Product	Time (min)	Yield[b] (%)
1			45	95
2			40	95
3			35	96
4			50	92
5			55	90
6			45	88
7			45	87
8			50	85
9			55	83
10			65	84
11			75	82
12			90	80
13			50	84
14			50	86

[a] Reaction condition: alcohol (1 mmol), DHP (1.2 mmol), catalyst (20 mol%), room temperature, solvent-free conditions. [b] Isolated yield.

Table 3 Competitive reactions of different binary mixtures[a]

Entry	Alcohols	Products	Time (min)	% Conversion
1			45	95
				5
2			45	100
				0
3			60	94
				6
4			60	100
				0

[a] Reaction condition: alcohol (1 mmol), DHP (1.2 mmol), catalyst (20 mol%), room temperature, solvent-free conditions.

In order to gain more insights into the selectivity of our method, we studied various competitive reactions between structurally different alcohols in binary mixtures as shown in Table 3. This study reveals that benzylic alcohols can be converted into their protected products with excellent selectivity in the presence of aliphatic alcohols (Table 3, entry 1). Interestingly, benzylic alcohols were converted quantitatively into their protected alcohols, while the secondary alcohol remained intact (Table 3, entry 2).

Allyl alcohols also reacted faster as compared to their aliphatic counterparts, affording the allyl products in high yield (Table 3, entry 3). Similarly, primary alcohols can also be converted to their corresponding THP ether in the presence of tertiary ones with complete selectivity (Table 3, entry 4).

Scheme 3 Proposed mechanism for the tetrahydropyranylation of alcohols using $Fe_3O_4@SiO_2@SO_3H$ nanocatalyst.
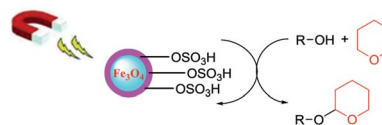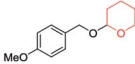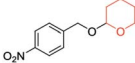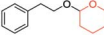
Fig. 4 Recyclability test of nanocatalyst for protection/deprotection of alcohols.

The mechanism proposed for the tetrahydropyranylation of alcohols catalyzed by $Fe_3O_4@SiO_2@SO_3H$ is shown in Scheme 3.
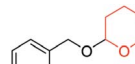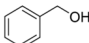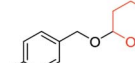
3.3 Recycling of the catalyst
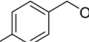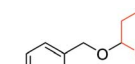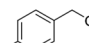
The recyclability of the magnetic nanocatalyst was investigated with consecutive tetrahydropyranylation reactions using different substrates. Fig. 4 depicts the results of consecutive runs performed by reusing the catalyst under our optimal reaction conditions. After each catalytic run, the catalyst was

Table 4 Reusability test of the catalyst under optimized reaction conditions[a]

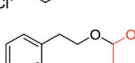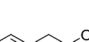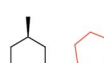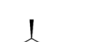| Entry	Products	Run/yield %					
1		Run	1	2	3	4	5
		Yield (%)	96	96	94	94	93
2		Run	1	2	3	4	5
		Yield (%)	90	89	89	89	88
3		Run	1	2	3	4	5
		Yield (%)	88	88	86	86	84

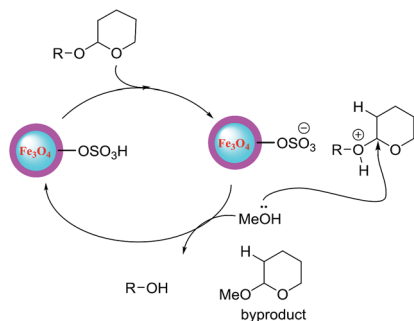[a] Reaction condition: alcohol (1 mmol), DHP (1.2 mmol), catalyst (20 mol%), room temperature.

Table 5 Deprotection of THP ethers

Entry	Alcohols	Product	Time (min)	Yield[a] (%)
1			25	95
2			30	92
3			25	95
4			20	90
5			30	90

[a] Reaction condition: THP ether (1 mmol), methanol (0.5 ml), catalyst (20 mol%), room temperature.

Scheme 4 Plausible mechanism for the deprotection/dehydropyranylation of THP ether.

recovered by an external magnet, washed with ethyl acetate and then dried at 100 °C in Abderhalden apparatus under reduced pressure overnight before being used again in a new reaction. We demonstrated that no depreciations in the catalytic performance were observed in all the test reactions even after five catalytic cycles. In addition, no difference in the IR spectrum of the catalyst was observed after these repeated cycles (Table 4).

3.4 Deprotection of THP ether

The deprotection of THP ethers was investigated by changing the solvent system. We found that the addition of methanol serves as an efficient deprotecting reagent for THP ethers in the presence of Fe_3O_4@silica sulfonic acid as a catalyst at room temperature to provide the corresponding free alcohols in an excellent yield of 90–95% (Table 5) irrespective of the structural variations. It is interesting to note that the deprotection of all the compounds reported in the present study was completed within 30 min. The proposed mechanism for the deprotection of THP ether is shown in Scheme 4.

4. Conclusions

Protection/deprotection is one of the most frequently applied synthetic strategies by organic chemists; discovery of more green and efficient heterogeneous catalysts for these reactions has been a fundamental necessity. The tetrahydropyranylation of alcohols using our reported magnetic Fe_3O_4@silica sulfonic acid nanocatalyst offers a green, mild, less toxic, stable, and solvent-free process of protection/deprotection reaction with easy recoverability of the catalyst. In short, our method is highly economical and environmentally benign.

5. Spectral data

5.1 2-((4-Methylbenzyl)oxy)-tetrahydro-2H-pyran (Table 2, entry 2)

^{1}H-NMR (400 MHz, CDCl$_3$, TMS): δ 7.27 (d, J = 8 Hz, 2H), 7.18 (d, J = 8 Hz, 2H), 4.79–4.71 (m, 2H), 4.50 (d, J = 12 Hz, 1H), 3.95–3.92 (m, 1H), 3.58–3.55 (m, 1H), 2.36 (s, 3H), 1.91–1.67 (m, 1H), 1.58–1.54 (m, 5H); ^{13}C-NMR (100 MHz, CDCl$_3$, TMS): δ 137.28, 135.34, 129.16, 128.09, 97.64, 68.27, 62.17, 30.71, 25.64, 21.29, 19.49.

5.2 2-(4-Methoxybenzyloxy)-tetrahydro-2H-pyran (Table 2, entry 3)

^{1}H-NMR (400 MHz, CDCl$_3$, TMS): δ 7.26–7.28 (d, J = 8 Hz, 2H), 6.84–6.86 (d, J = 8 Hz, 2H), 4.66–4.71 (m, 2H), 4.43 (d, J = 4 Hz, 1H), 3.90 (t, J = 4 Hz, 1H), 3.74 (s, 3H), 3.53 (t, J = 4 Hz, 1H), 1.49–1.83 (m, 6H); ^{13}C-NMR (100 MHz, CDCl$_3$, TMS): δ 159.24, 130.37, 129.56, 113.81, 97.49, 68.53, 62.11, 55.21, 30.70, 25.61, 25.57, 19.50.

5.3 Tetrahydro-2-(phenethyloxy)-2H-pyran (Table 2, entry 6)

^{1}H-NMR (400 MHz, CDCl$_3$, TMS): δ 7.13–7.25 (m, 4H), 4.56 (t, J = 3.6 Hz, 1H), 3.38–3.95 (m, 4H), 2.88 (t, J = 7.2 Hz, 2H), 1.42–1.82 (m, 7H); ^{13}C-NMR (100 MHz, CDCl$_3$, TMS): δ 139.15, 128.76, 126.25, 98.614, 68.291, 62.8, 39.38, 36.446, 30.712, 25.546, 19.63.

5.4 2-(2-Ethylhexyloxy)-tetrahydro-2H-pyran (Table 2, entry 7)

^{1}H-NMR (400 MHz, CDCl$_3$, TMS): δ 4.51–4.52 (t, J = 4 Hz, 1H), 3.58–3.81 (m, 2H), 3.18–3.56 (m, 2H), 1.48–1.77 (m, 7H), 1.24–1.29 (m, 8H), 0.82–0.86 (m, 6H); ^{13}C-NMR (100 MHz, CDCl$_3$, TMS): δ 99.04, 98.93, 70.4, 62.08, 39.73, 39.66, 30.79, 30.61, 29.17, 29.13, 25.62, 23.94, 23.14, 19.57, 14.13, 11.17, 11.06.

5.5 2-(8-Methylnonyloxy)-tetrahydro-2H-pyran (Table 2, entry 8)

^{1}H-NMR (400 MHz, CDCl$_3$, TMS): δ 4.572 (s, 1H), 3.72–3.88 (m, 2H), 3.49 (d, J = 12 Hz, 2H), 1.40–1.84 (m, 19H), 1.07–1.33 (m, 10H); ^{13}C-NMR (100 MHz, CDCl$_3$, TMS): δ 19.45, 22.74, 25.26, 26.68, 27.14, 27.80, 29.24, 29.81, 30.62, 41.04, 62.13, 67.38, 98.47.

5.6 2-(Octyloxy)-tetrahydro-2H-pyran (Table 2, entry 9)

^{1}H-NMR (400 MHz, CDCl$_3$, TMS): δ 4.54 (t, J = 4 Hz, 1H), 3.83–3.70 (m, 1H), 3.69–3.66 (m, 1H), 3.51–3.47 (m, 1H), 3.35–3.32 (m, 1H), 1.78–1.55 (m, 1H), 1.53–1.51 (m, 1H), 1.51–1.48 (m, 6H), 1.32–1.23 (m, 11H), 0.85 (t, J = 8 Hz, 3H); ^{13}C-NMR (100 MHz, CDCl$_3$, TMS): δ 98.87, 67.74, 62.34, 31.91, 30.84, 29.82, 29.53, 26.32, 25.58, 22.73, 19.74, 14.16.

Conflicts of interest

There are no conflicts of interest to declare.

Acknowledgements

References

1 B. Kumar, M. A. Aga, D. Mukherjee, S. S. Chimni and S. C. Taneja, *Tetrahedron Lett.*, 2009, **50**, 6236.
2 T. W. Greene and P. G. M. Wuts, in *Protective Groups in Organic Synthesis*, John Wiley & Sons, New York, 2007.

3 D. B. G. Williams, S. B. Simelane, M. Lawton and H. H. Kinfe, *Tetrahedron*, 2010, **66**, 4573.

4 M. Miyashita, A. Yoshikoshi and P. A. Grieco, *J. Org. Chem.*, 1977, **42**, 3774.

5 T. Sato, J. Otera and H. Nozaki, *J. Org. Chem.*, 1990, **55**, 4770.

6 H. Firouzabadi, N. Iranpoor and H. Hazarkhani, *Tetrahedron Lett.*, 2002, **43**, 7139.

7 S. Kim and W. J. Lee, *Synth. Commun.*, 1986, **16**, 659.

8 B. Akhlaghinia, *Phosphorus, Sulfur Silicon Relat. Elem.*, 2004, **179**, 1783.

9 M. Yadegari and M. Moghadam, *Appl. Organomet. Chem.*, 2016, **30**, 872.

10 B. Karimi and M. Khalkhali, *J. Mol. Catal. A: Chem.*, 2005, **232**, 113.

11 R. A. Sheldon and R. S. Downing, *Appl. Catal., A*, 1999, **189**, 163.

12 B. F. G. Johnson, *Top. Catal.*, 2003, **24**, 147.

13 A. K. Rathi, R. Zboril, R. S. Varma and M. B. Gawande, in *Magnetite (Ferrites)-Supported Nano-Catalysts: Sustainable Applications in Organic Transformations, ACS Symposium Series*, ACS, Washington DC, 2016, ch. 2, p. 39.

14 L. M. Liz-Marzin and P. Mulvaney, *J. Phys. Chem. B*, 2003, **107**, 7312.

15 O. B. Miguel, P. Tartaj, M. P. Morales, P. Bonville, U. G. Schindler, X. Q. Zhao and S. V. Verdaguer, *Small*, 2006, **2**, 1476.

16 B. Dam, A. Kumar Pal and A. Gupta, *Synth. Commun.*, 2016, **46**, 275.

17 J. Safari and Z. Zarnegar, *J. Mol. Catal. A: Chem.*, 2013, **379**, 269.

18 A. Rostami, A. Ghorbani-Choghamarani, B. Tahmasbi, F. Sharifi, Y. Navasi and D. Moradi, *J. Saudi Chem. Soc.*, 2017, **21**, 399.

19 A. R. Kiasat and J. Davarpanah, *J. Mol. Catal. A: Chem.*, 2013, **373**, 46.

20 H. Naeimi and S. Mohamadabadi, *Dalton Trans.*, 2014, **43**, 12967.

21 F. Nemati, M. M. Heravi and R. Saeedirad, *Chin. J. Catal.*, 2012, **33**, 1825.